Supplementary Information

Carbon Dioxide - Sulphur Hexafluoride Adsorption and Separation with Zirconium Metal-Organic Frameworks Bearing Basic and Fluorinated Linkers

Giacomo Provinciali,[a] Giulio Bicchierai,[a] Ferdinando Costantino,[b] Cristiano Zuccaccia,[b] Letizia Trovarelli,[b,c] Lorenzo Donà,[c] Bartolomeo Civalleri,[c] Francesca Bonino,[c] Francesca Rosso,[c] Giuliano Giambastiani,[d,e,a] Giulia Tuci,[a,e] and Andrea Rossin[a,e]*

[a] Istituto di Chimica dei Composti Organometallici (CNR-ICCOM), Via Madonna del Piano 10, Sesto Fiorentino (Firenze), 50019, Italy. E-mail: a.rossin@iccom.cnr.it

[b] Dipartimento di Chimica, Biologia e Biotecnologie e CIRCC, Università degli Studi di Perugia, via Elce di Sotto 8, 06123 Perugia, Italy.

[c] Dipartimento di Chimica, Centro NIS, Unità di Ricerca INSTM, Università di Torino, Via G. Quarello 15/A and Via P. Giuria 7, I-10125 Torino, Italy.

[d] Dipartimento di Chimica Ugo Schiff, Università di Firenze, Via della Lastruccia 3-13, 50019 Sesto Fiorentino (Firenze), Italy.

[e] Consorzio Interuniversitario Nazionale per la Scienza e Tecnologia dei Materiali (INSTM), Via G. Giusti, 9 50121 Firenze, Italy.

Experimental determination of Zr_TFA_NH_2 and Zr_TFA_PyPy molecular formulae through quantitative ^{1}H- and ^{19}F-NMR spectroscopy

A standard solution was prepared by dissolving 5.5 mg of 2-aminoterephtalic acid (for ^{1}H NMR quantification, Fig. S1a) and 7.7 mg of 2,3,5,6-tetrafluoroterephtalic acid (for ^{19}F NMR quantification, Fig. S1d) in 1.5 mL of D_2SO_4/D_2O(96% w/w)/DMSO-d_6 to give a nominal concentration equal to 20 mM for each solute. Quantitative integration of the ^{1}H NMR spectrum for the solution of digested **Zr_TFA_NH_2** gives a concentration of 2-aminoterephthalic acid equal to 4.8 mM (Fig. S1b). A sharp singlet at $\delta_F = -76.06$ ppm in the ^{19}F-NMR spectrum was observed and attributed to trifluoroacetic acid (Fig. S1e). The concentration of the latter was found to be 5.2 mM. The resulting molar ratio [H_2BDC-NH_2]/[HTFA] = mol(H_2BDC-NH_2)/mol(HTFA) = 4.8/5.2 equals 0.92. Assuming the general formula [$Zr_6O_4(OH)_4$(BDC-NH_2)$_{6-x}$(TFA)$_{2x}$], the proposed experimental formula for **Zr_TFA_NH_2** is [$Zr_6O_4(OH)_4$(BDC-NH_2)$_{3.9}$(TFA)$_{4.2}$].

Following the same approach for **Zr_TFA_PyPy**, quantitative integration of the ^{1}H NMR spectrum for the digested solution gives a concentration of [2,2′-bipyridine]-4,4′-dicarboxylic acid equal to 6.3 mM (Fig. S1c). Again, the signal of trifluoroacetic acid at $\delta_F = -76.06$ ppm was observed in the ^{19}F NMR spectrum (Fig. S1f). The concentration of trifluoroacetic acid was found to be 2.2 mM, affording the experimental formula [$Zr_6O_4(OH)_4$(PyPy)$_{5.1}$(TFA)$_{1.8}$] for **Zr_TFA_PyPy**.

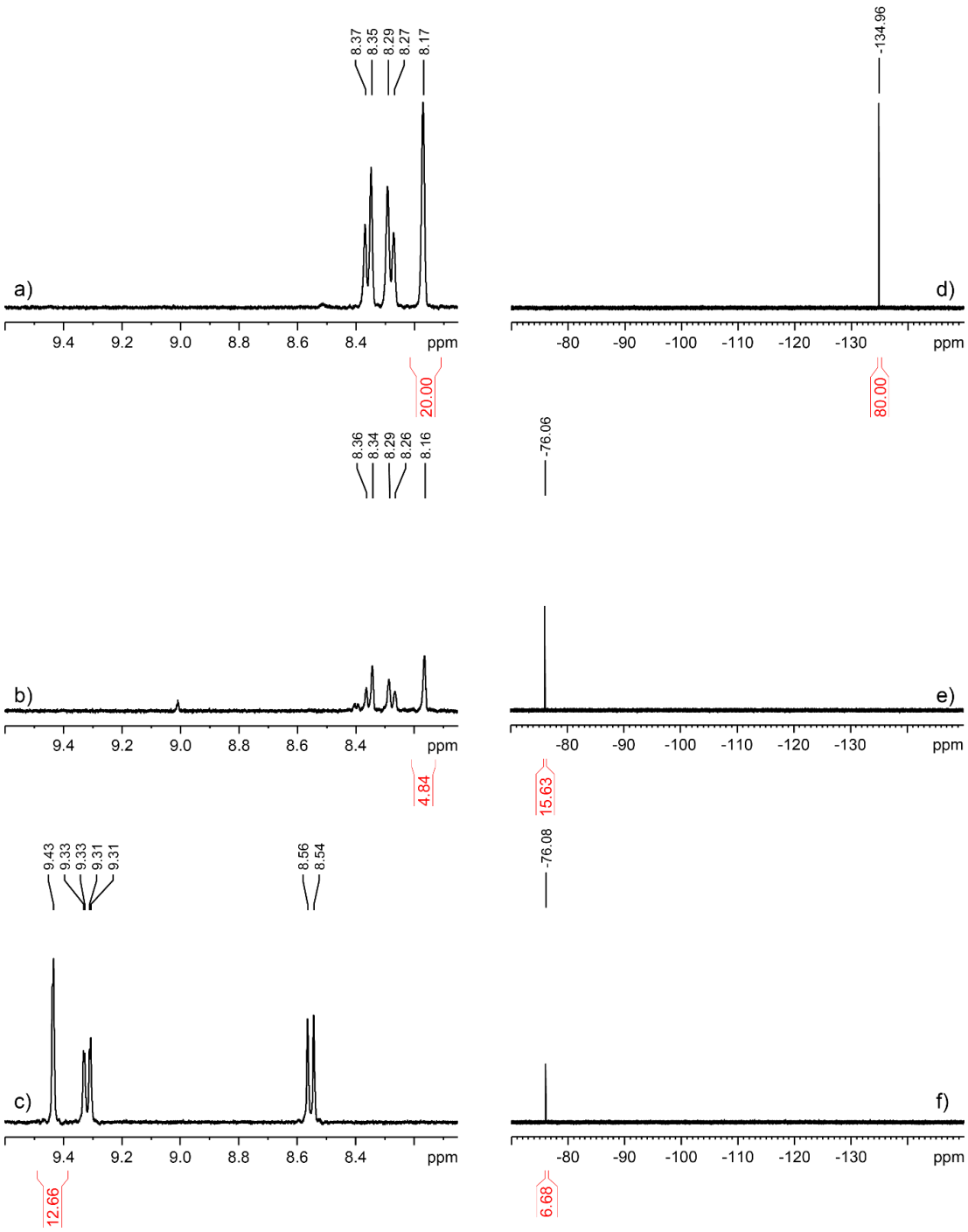

Fig. S1. Top: ^{1}H (a) and ^{19}F (d) NMR spectra of the standard solution containing 2-aminoterephtalic acid (20 mM) and 2,3,5,6-tetrafluoroterephtalic acid (20 mM). Middle: ^{1}H (b) and ^{19}F (e) NMR spectra the solution from digestion of **Zr_TFA_NH$_2$**. Bottom: ^{1}H (c) and ^{19}F (f) NMR spectra the solution from digestion of **Zr_TFA_PyPy**. Integral values for (b) and (c) are relative to spectrum (a); integral values for (e) and (f) are relative to spectrum (d).

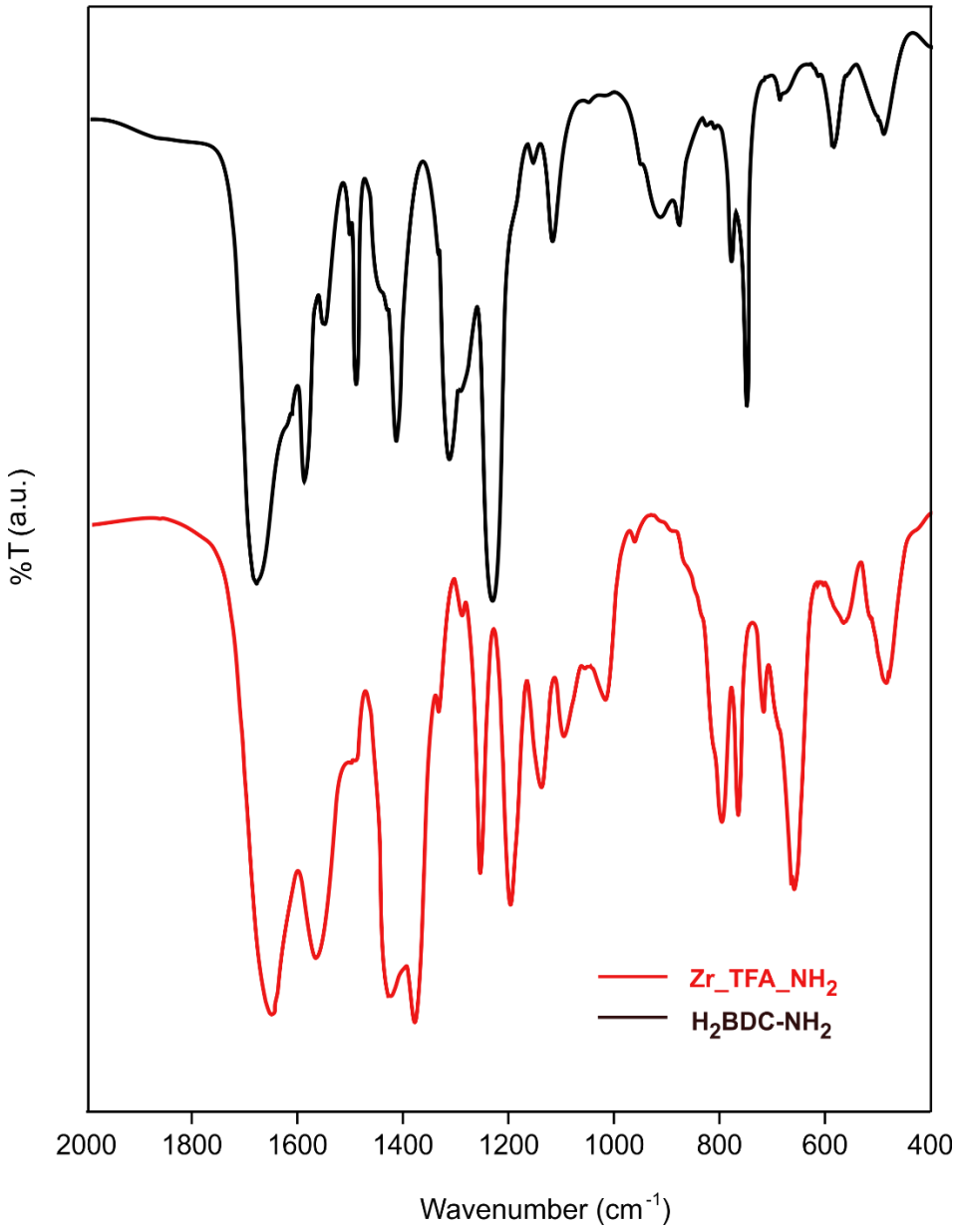

Fig. S2. Infrared spectra (KBr, T = 298 K, 2000-400 cm^{-1}) of **Zr_TFA_NH₂** and its constitutive linker $H_2BDC\text{-}NH_2$ at comparison.

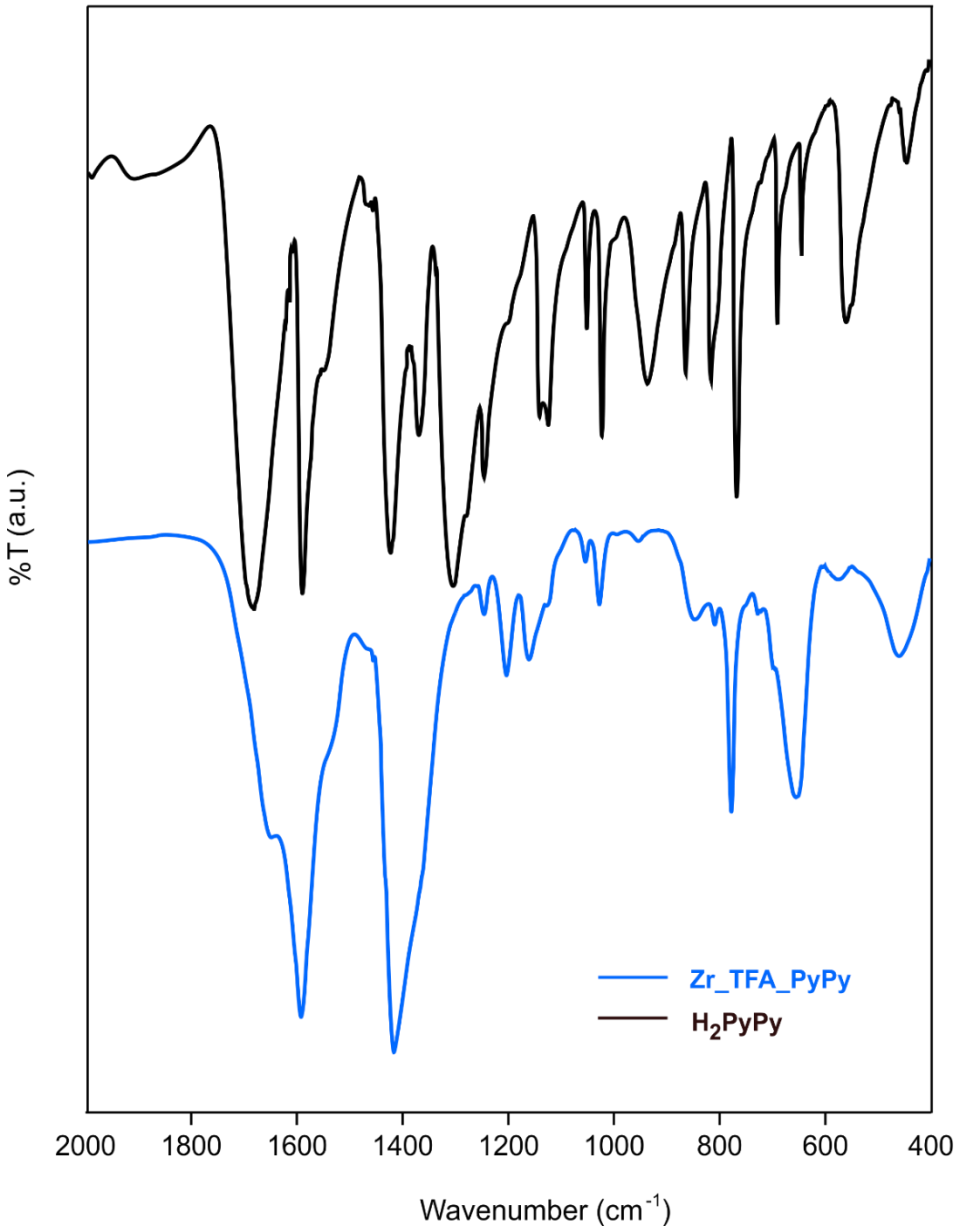

Fig. S3. Infrared spectra (KBr, T = 298 K, 2000-400 cm^{-1}) of **Zr_TFA_PyPy** and its constitutive linker H_2PyPy at comparison.

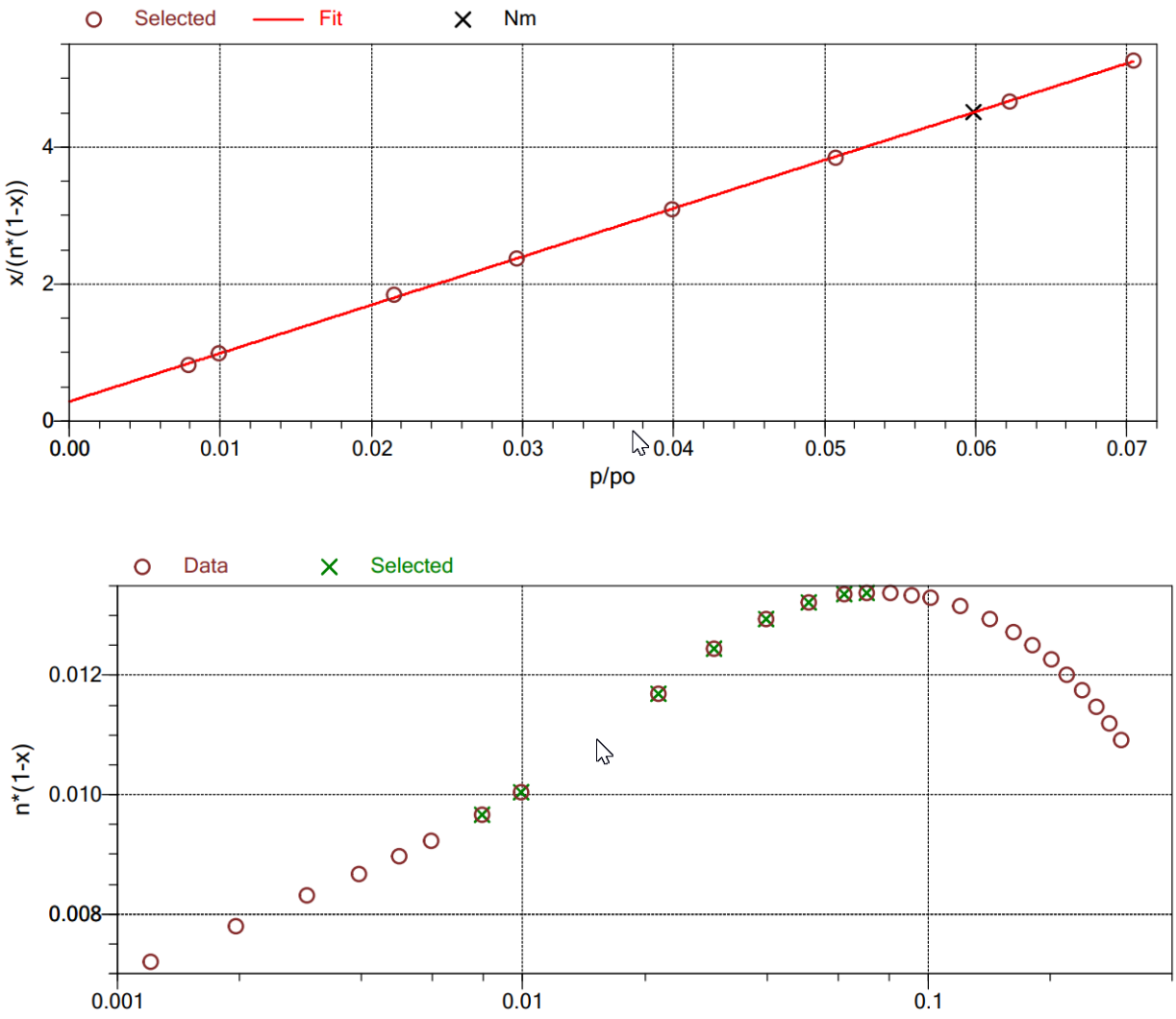

Fig. S4. BET linear plot and Rouquerol transform on the N_2 isotherm collected at T = 77 K of **Zr_TFA_NH$_2$**. C = 247; R^2 = 0.99983.

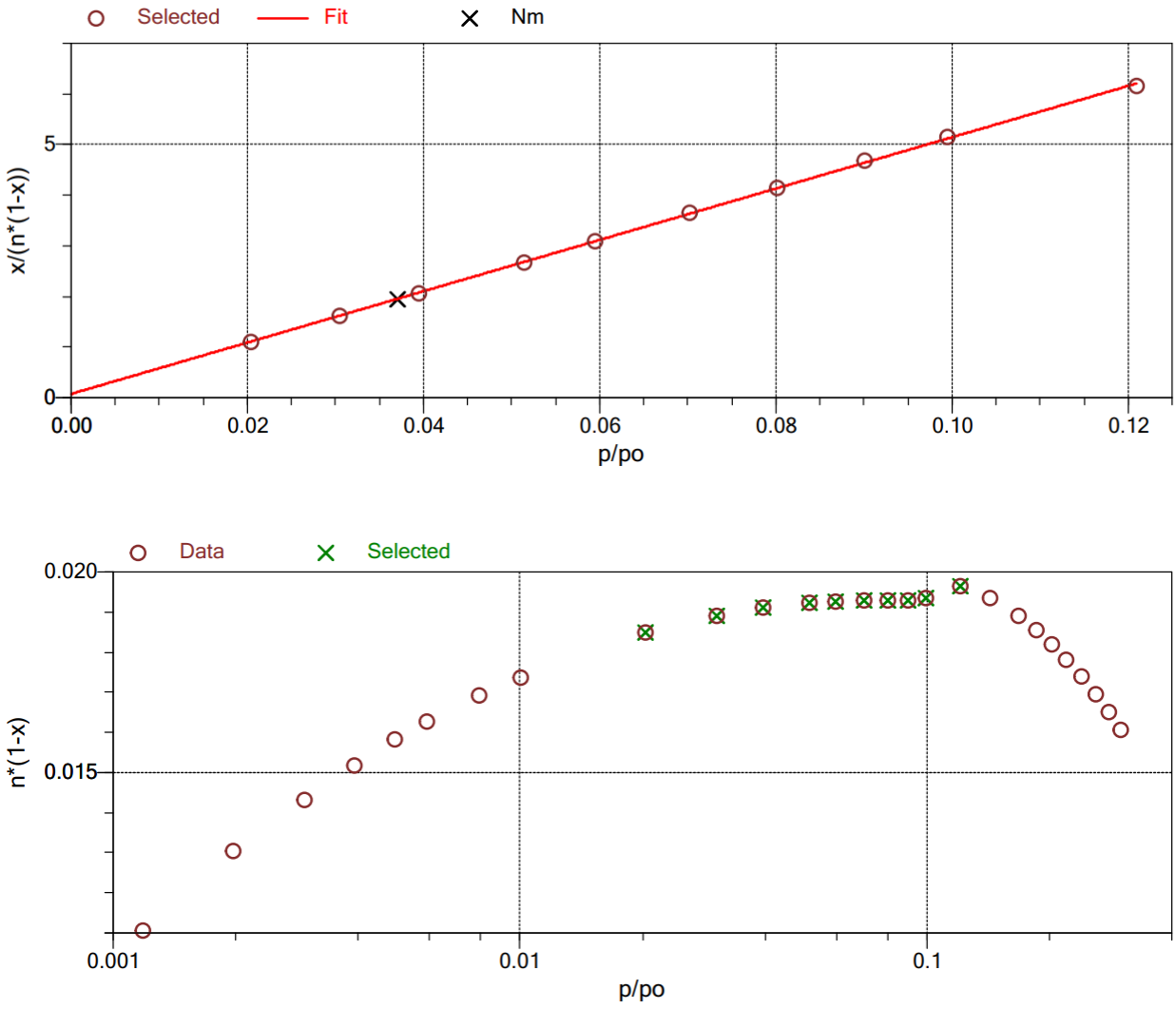

Fig. S5. BET linear plot and Rouquerol transform on the N_2 isotherm collected at T = 77 K of **Zr_TFA_PyPy**. C = 678; R^2 = 0.99982.

Details of the calculation in breakthrough experiments

The samples were weighted in air directly in the quartz reactor. The amount of sample was subsequently corrected by the loss percentage in the TGA curves at 423 K.The data obtained from the mass spectrometer were corrected using the Ar costant flow, to account for the possible pressure variation during the experiment. The mass data were used to calculate the outlet molar fraction ($y_i(t)$, i = He, Ar, CO_2 or SF_6) of each component. The outlet total volumetric flow [$\dot{Q}_{tot}(t)$] was estimated by means of $y_{He,out}$ and its inlet volumetric flow ($\dot{Q}_{He,in}$):

$$\dot{Q}_{tot}(t) = \frac{\dot{Q}_{He,in}}{y_{He}(t)}$$

For each experiment (with both sample and empty reactor), the mmol retained (n_i) were calculated using the following equation from the adsorption branch:

$$n_i = \dot{n}_{i,in} \int_0^{\infty} \left(1 - \frac{\dot{Q}_{tot}(t) * y_i(t)}{\dot{Q}_{tot,in} * y_{i,in}}\right)$$

And with the following equation from the desorption branch:

$$n_i = \dot{n}_{i,init} \int_0^{\infty} \left(\frac{\dot{Q}_{tot}(t) * y_i(t)}{\dot{Q}_{tot,init} * y_{i,init}}\right)$$

Where $\dot{Q}_{tot,init}$ (mL/min) and $y_{i,init}$ are the total volumetric flow and the molar fraction of *i* used during the adsorption run. The inlet molar flow, $\dot{n}_{i,in}$, (mmol/min) was calculated as reported below from the inlet (or initial) volumetric flow:

$$\dot{n}_{i,in} = \frac{\dot{Q}_{tot,in}}{\tilde{V}_i}$$

In this equation, the molar volume $\tilde{V}_i$ is calculated as it follows:

$$\tilde{V}_i = \frac{Z\ R\ T}{p}$$

Where *R* is the ideal gas constant, *T* is the temperature, *p* is the pressure and *Z* is the compressibility factor. *Z* values at T = 298 K and p = 1.013 bar are 0.9950 and 0.9887 for CO_2 and SF_6, respectively (https://encyclopedia.airliquide.com/).

The amount adsorbed (q_i) was hence calculated both from the adsorption and desorption branch, using the following equation:

$$q_i = \frac{n_{i,exp} - n_{i,blank} - \frac{m_{smp}}{\rho_{smp} * \tilde{V}_i}}{m_{smp}}$$

Where $n_{i,exp}$ are the mmol retained during the experiment with the sample, $n_{i,blank}$ are the mmol retained during the experiment performed with the empty reactor, m_{smp} is the mass of sample (corrected by the TGA), ρ_{smp} is the pycnometric density of the sample and $\tilde{V}_i$ is the molar volume, calculated taking into account the Z factor reported above. Given the relatively small amount adsorbed and the full reversibility of the adsorption process already at ambient temperature and pressure, the quantification was performed using the desorption branch, as indicated in the relevant literature.[1] The selectivity was obtained as reported in the main text for the IAST calculation.

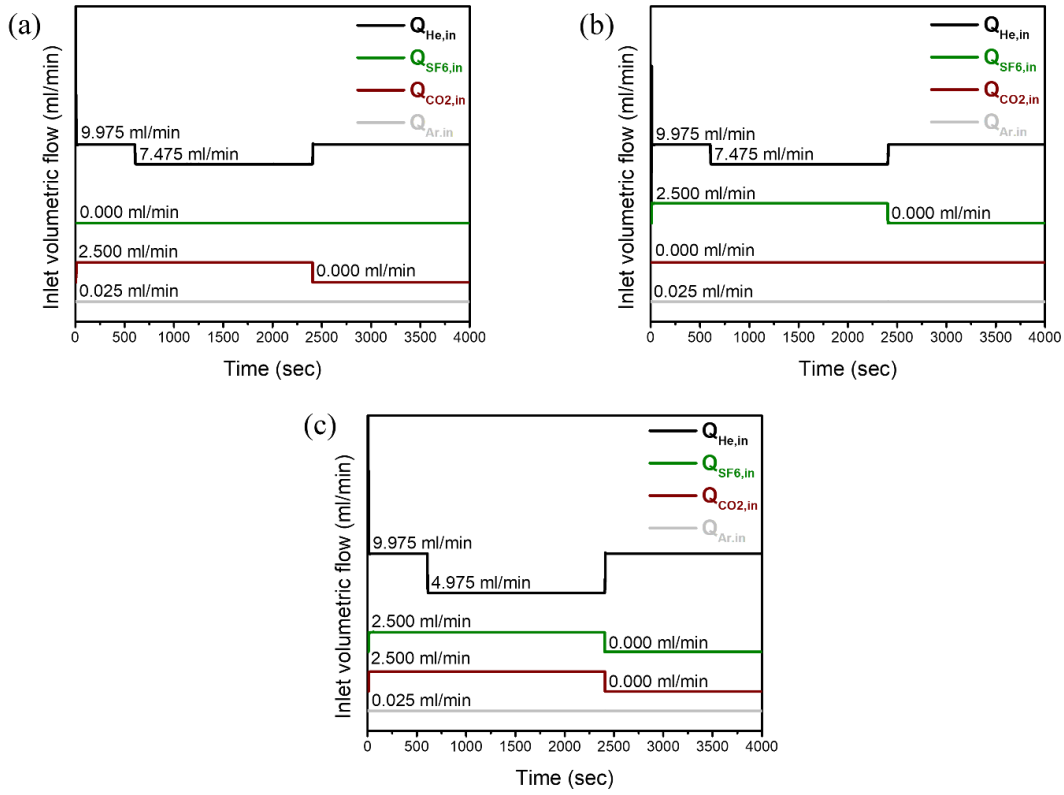

Fig. S6. Schematic of the inlet volumetric flow used in BT experiments where CO_2 only (a), SF_6 only (b) and CO_2 and SF_6 competitive (c) sorption were performed. The time of the two knees in the He flows signal corresponds to the start time of the adsorption and desorption runs respectively.

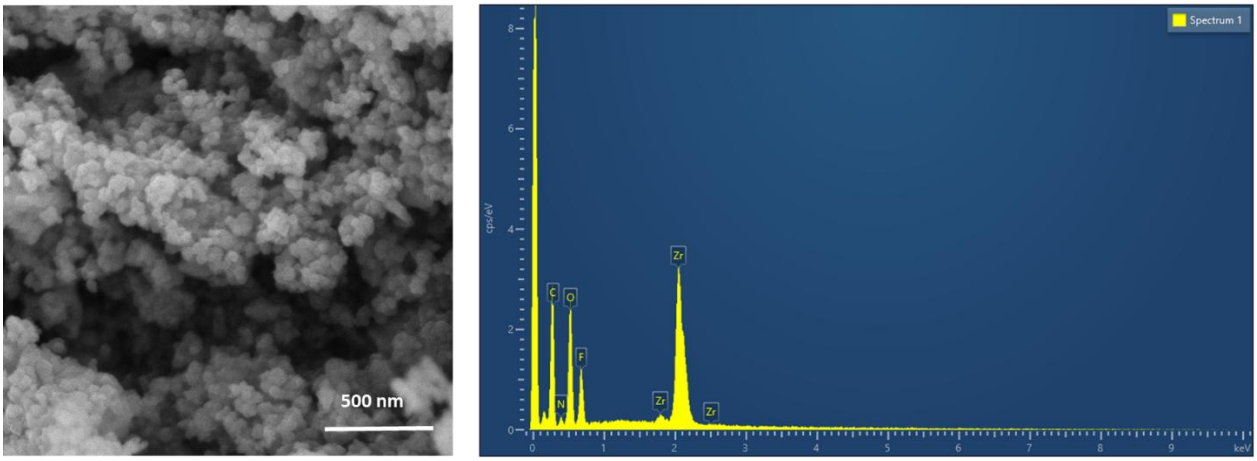

Fig. S7. FE-SEM images and related EDX analysis of **Zr_TFA_NH$_2$**.

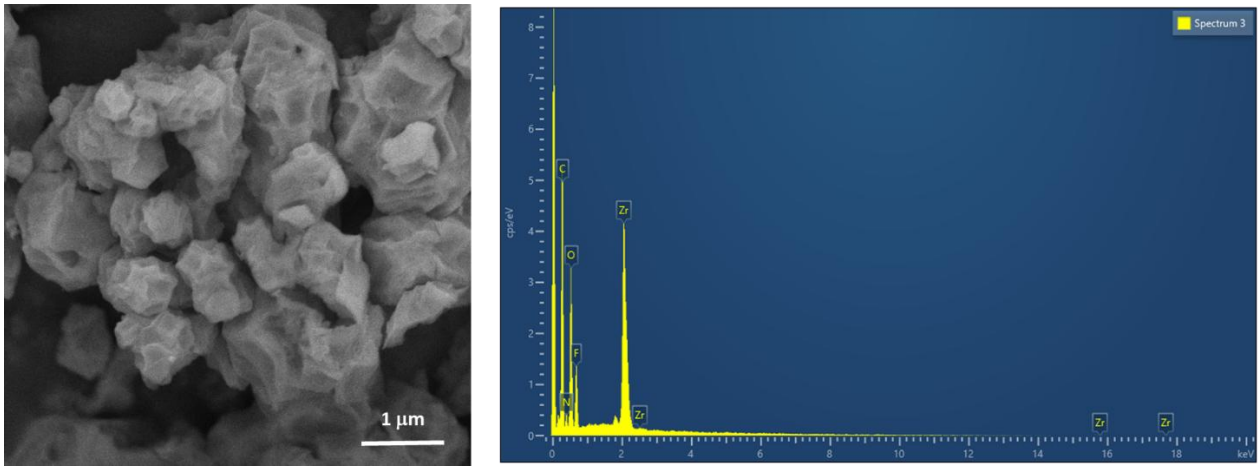

Fig. S8. FE-SEM images and related EDX analysis of **Zr_TFA_PyPy**.

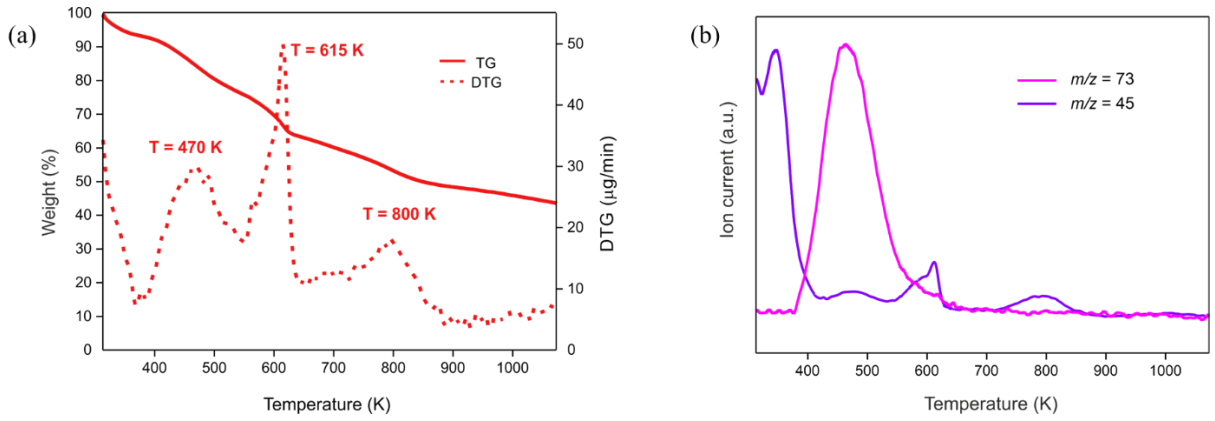

Fig. S9. TG-DTG traces (a) and related mass spectrometry peaks (b) of **Zr_TFA_NH$_2$**.

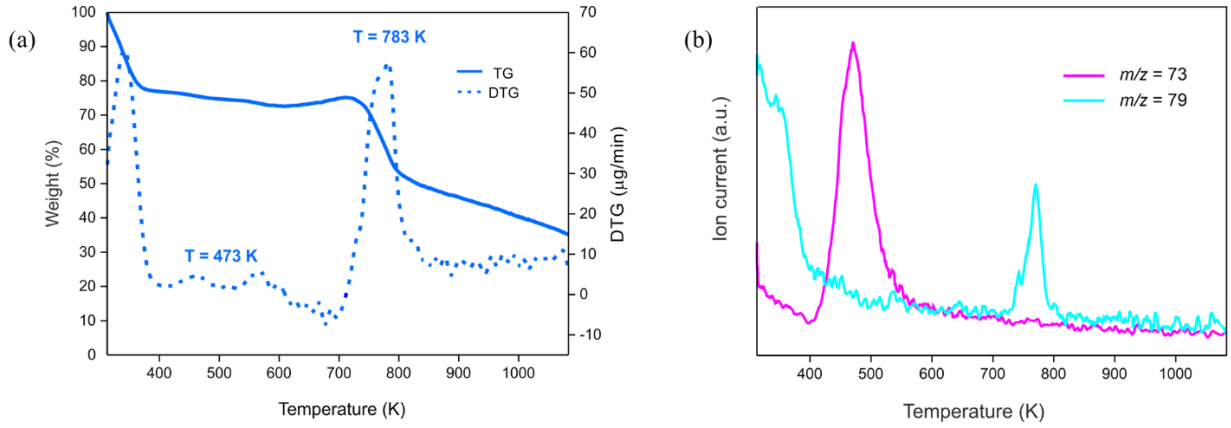

Fig. S10. TG-DTG traces (a) and related mass spectrometry peaks (b) of **Zr_TFA_PyPy**.

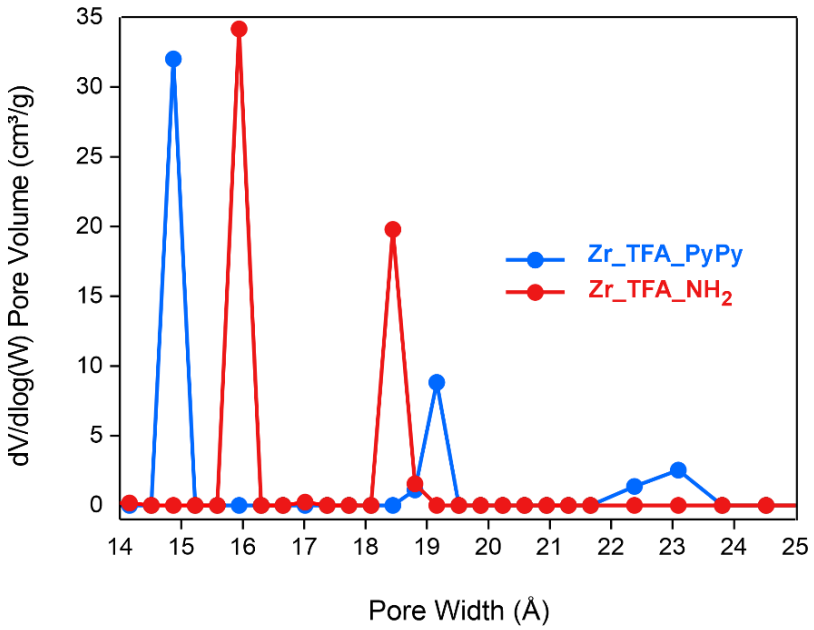

Fig. S11. Micropore size distribution (NLDFT method – Tarazona approximation, cylindrical pore shape) of **Zr_TFA_NH2** and **Zr_TFA_PyPy** at comparison.

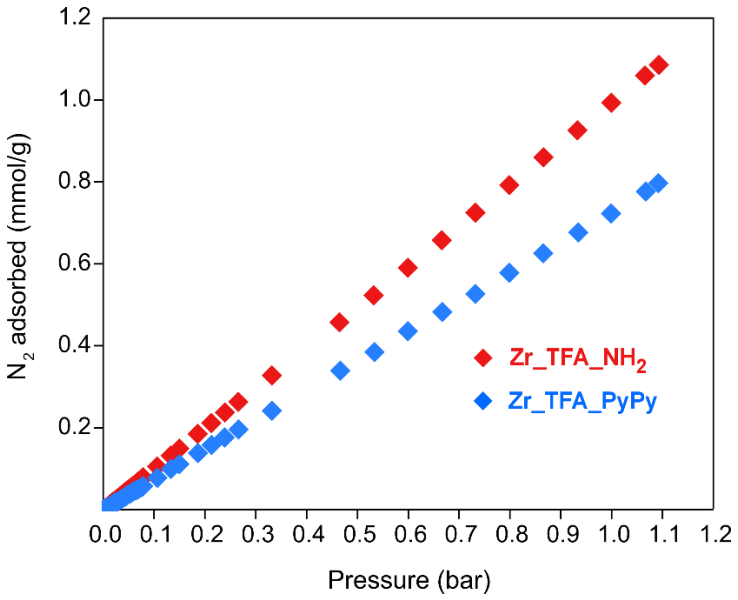

Fig. S12. N_2 adsorption isotherms collected at T = 298 K of **Zr_TFA_NH2** and **Zr_TFA_PyPy** at comparison.

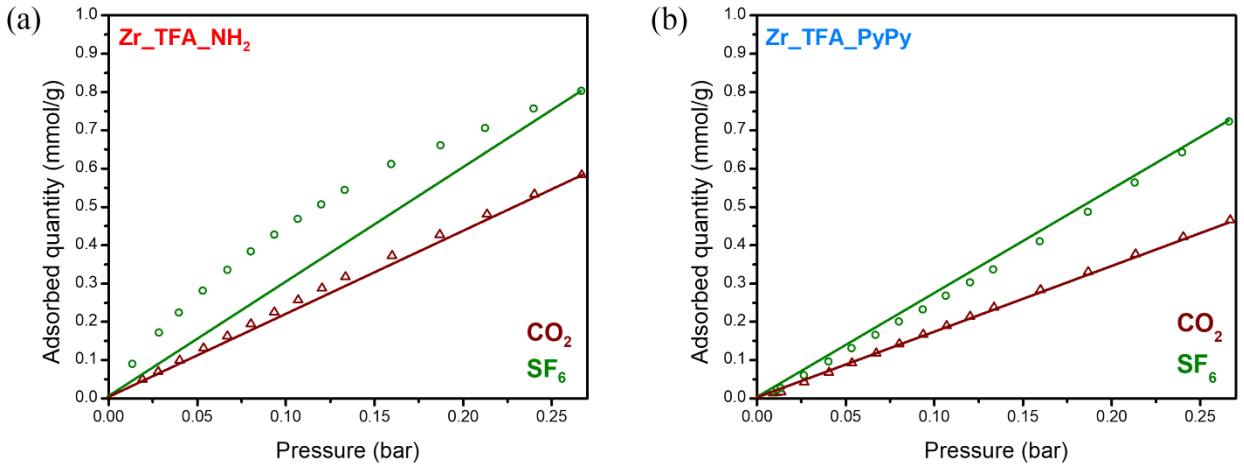

Fig. S13. Inset of the adsorption isotherms (empty symbols) of CO_2 and SF_6 on (a) **Zr_TFA_NH2** and (b) **Zr_TFA_PyPy**. The straight lines connect the origin of the graph with the isotherm point at 0.26 bar, to highlight the more or less linear isotherm shape.

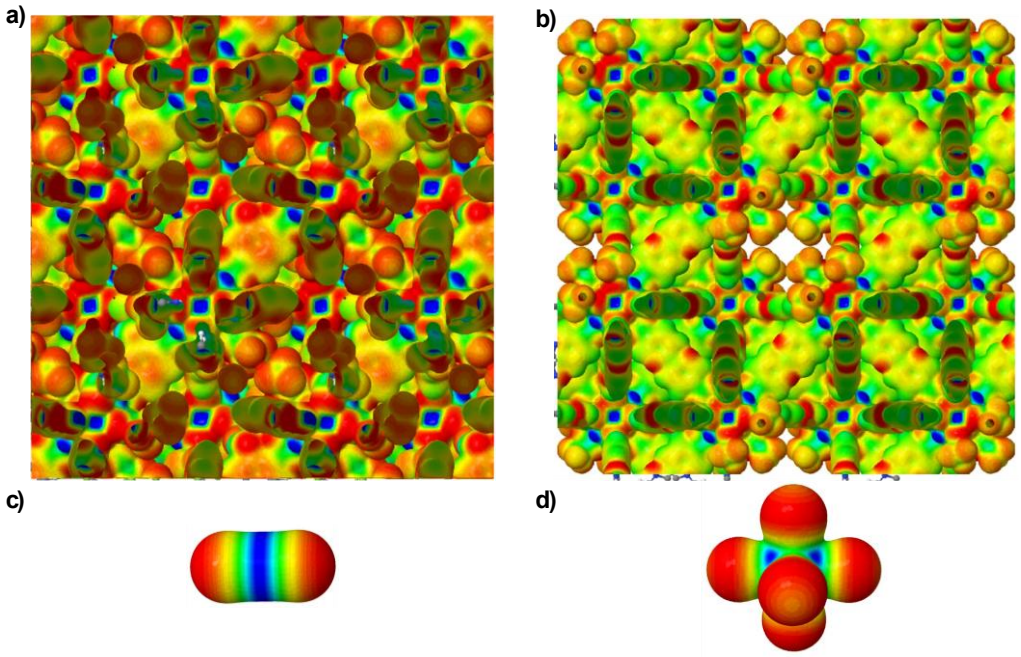

Fig. S14. Electrostatic potential mapped on an electron density isosurface of 0.003 |e| (positive regions in blue and negative regions in red) for **Zr_TFA_NH2** (a), **Zr_TFA_PyPy** (b), CO_2 (c) and SF_6 (d).

Table S1. Comparison of the SF_6 and CO_2 adsorption performance of **Zr_TFA_NH2** and **Zr_TFA_PyPy** with other Zr^{IV} MOFs from the literature.

MOF	SSA [m^2/g]	Qst (SF_6) [kJ/mol]	Qst (CO_2) [kJ/mol]	Reference
Zr_TFA_NH2	1380	31	29	This work
Zr_TFA_PyPy	1922	23	28	This work
UiO-66	1333	33	22	[2/3]
UiO-66-Br	759	35	23	[4/5]
UiO-66-Br_2	616	45	--	[4]
UiO-66-Cl	752	32	--	[4]
UiO-66-I	819	38	--	[4]
UiO-66-NH_2	938	32	25	[4/3]
UiO-66-NO_2	774	35	30	[4/5]
UiO-67	2411	20	16	[6/7]
Zr_PyPy	2273	--	21	[8]

Table S2. Comparison between calculated PBEsol0-3c interaction energies (kJ/mol) for CO_2 and SF_6 in **Zr_TFA_NH2** on different binding sites (in bold the calculated preferential adsorption site) and the experimental isosteric heats of adsorption.

	CF_3	**NH_2**	**OH**	**Zr**	**Experimental Q_{st}**
CO_2	-28.12	**-33.22**	-27.90	-27.86	29
SF_6	-32.85	-29.88	**-37.05**	-32.87	31

Table S3. Comparison between calculated PBEsol0-3c interaction energies (kJ/mol) for CO_2 and SF_6 in **Zr_TFA_PyPy** on different binding sites (in bold the calculated preferential adsorption site) and the experimental isosteric heats of adsorption.

	CF_3	**N(PyPy)**	**OH**	**Zr**	**Experimental Q_{st}**
CO_2	-23.98	-18.38	-24.90	**-26.98**	28
SF_6	-3.62	-23.86	**-25.64**	-24.71	23

References

1. N. S. Wilkins, A. Rajendran and S. Farooq, *Adsorption*, 2021, **27**, 397–422.
2. M.-B. Kim, T.-U. Yoon, D.-Y. Hong, S.-Y. Kim, S.-J. Lee, S.-I. Kim, S.-K. Lee, J.-S. Chang and Y.-S. Bae, *Chem. Eng. J.*, 2015, **276**, 315–321.
3. J. Ethiraj, E. Albanese, B. Civalleri, J. G. Vitillo, F. Bonino, S. Chavan, G. C. Shearer, K. P. Lillerud and S. Bordiga, *ChemSusChem*, 2014, **7**, 3382–3388.
4. M.-B. Kim, K.-M. Kim, T.-H. Kim, T.-U. Yoon, E.-J. Kim, J.-H. Kim and Y.-S. Bae, *Chem. Eng. J.*, 2018, **339**, 223–229.
5. Y. Huang, W. Qin, Z. Li and Y. Li, *Dalton Trans.*, 2012, **41**, 9283–9285.
6. M.-B. Kim, T.-H. Kim, T.-U. Yoon, J. H. Kang, J.-H. Kim and Y.-S. Bae, *J. Ind. Eng. Chem.*, 2020, **84**, 179–184.
7. B. Wang, H. Huang, X.-L. Lv, Y. Xie, M. Li and J.-R. Li, *Inorg. Chem.*, 2014, **53**, 9254–9259.
8. S. Demir, N. Bilgin, H. M. Cepni, H. Furukawa, F. Yilmaz, C. Altintas and S. Keskin, *Dalton Trans.*, 2021, **50**, 16587–16592.